Hypoxia-Induced Cardiomyocyte Apoptosis Exacerbates Cardiomyocyte Hypertrophy and Myocardial Injury through p38 MAPK Pathway in SD Rats

Xiaoxu Li [ξ], Zhijun Pu [ξ], Gang Xu, Yidong Yang, Yu Cui, Xiaoying Zhou, Chenyuan Wang, Zhifeng Zhong, Simin Zhou, Jun Yi, Fabo Shan, Chengzhong Yang, Li Jiao [*], Dewei Chen [*], Jian Huang [*]

Posted Date: 16 February 2023

doi: 10.20944/preprints202302.0276.v1

Keywords: Hypoxia; p38; Apoptosis; Cardiomyocyte Hypertrophy; Myocardial Injury

Article

Hypoxia-Induced Cardiomyocyte Apoptosis Exacerbates Cardiomyocyte Hypertrophy and Myocardial Injury through p38 MAPK Pathway in SD Rats

Xiaoxu Li [1,2,3,†], Zhijun Pu [1,2,3,†], Gang Xu [2,3], Yidong Yang [1,2,3], Yu Cui [1,2,3], Xiaoying Zhou [1,2,3], Chenyuan Wang [1,2,3], Zhifeng Zhong [2,3], Simin Zhou [2,3], Jun Yin [2,3], Fabo Shan [4], Chengzhong Yang [1,2,3], Li Jiao [1,2,3,*], Dewei Chen [1,2,3,*] and Jian Huang [1,2,3,*]

[1] Department of High Altitude Physiology & Pathology, College of High Altitude Military Medicine, Army Medical University (Third Military Medical University), Chongqing 400038, China
[2] Key Laboratory of Extreme Environmental Medicine, Ministry of Education of China, Chongqing 400038, China
[3] Key Laboratory of High-Altitude Medicine, PLA, Chongqing 400038, China
[4] State Key Laboratory of Trauma, Burn and Combined Injury, Da-ping Hospital, Army Medical University, Chongqing, China
* Correspondence: 36705487@qq.com (L.J.); cdw528913@163.com (D.C.); huang3red@163.com (J.H.)
† Contribute to the same.

Abstract: Right ventricular remodeling and its function are closely related to the symptom severity and survival of hypoxia pulmonary hypertension, but molecular mechanisms of cardiomyocyte hypertrophy and myocardial injury remain unclear. It evaluated the cardiac function (by right cardiac catheterization to measure right ventricular systolic pressure and mean pulmonary artery pressure), myocardial tissue morphology (Haematoxylin and Eosin), myocardial hypertrophy (Wheat Germ Agglutinin Staining) , then RNA sequencing was applied to explore the mechanism, which results were verified by western blot in final. Hypoxia developed pulmonary hypertension, right ventricular diastolic and systolic functions were enhanced in rats, such as the mean pulmonary artery pressure, systolic pressure of pulmonary artery, the max pressure of right ventricular, the mean right ventricular pressure, and the heart rate was significantly higher than that in control. We found that HIF-1 signaling pathway and p38-MAPK signaling pathway have been activated by hypoxia, and cardiomyocyte apoptosis also aggravated in the right ventricular, which might be one cause of cardiomyocyte hypertrophy and myocardial injury, and targeted intervention might be one potential prevention for cardiomyocyte hypertrophy and myocardial injury induced by hypoxia.

Keywords: hypoxia; p38; apoptosis; cardiomyocyte hypertrophy; myocardial Injury

1. Introduction

Continuous hypoxia, such as hypoxia pulmonary hypertension, can change pulmonary vascular structure, increasing vascular hardness, reducing arterial lumen diameter and increasing blood flow resistance [1]. Hypoxic pulmonary vasoconstriction and vascular remodeling, along with increased right ventricle and blood viscosity, constitute components of hypoxia induced pulmonary hypertension (HPH), which increases the workload of the right ventricle, the current treatments are effective in improving symptoms, hemodynamics and functional capacity [2,3]; however, despite treatment, many patients live with persistent symptoms, even develop right heart failure or death. Approximately 140 million people live above 2500 m, and more 40 million people visit these regions every year [4,5]. It is a growing public health concern, and remained to be solved.

 doi:10.20944/preprints202302.0276.v1

Studies have shown that right ventricular remodeling and its function are closely related to symptom severity and survival of HPH [6–8]. Increased cardiac afterload and right ventricular remodeling due to chronic hypoxia result in a series of adaptive changes in shape, size, and structure that may contribute to right ventricular dysfunction, which is a complicated process that leads to inflammation, angiogenesis, fibrosis, and cardiac myocyte hypertrophy. Right ventricular adaptation to pulmonary hypertension is the main determinant of prognosis in patients with hypoxic pulmonary hypertension [9]. However, the underlying molecular mechanisms of right ventricular remodeling and dysfunction remain unclear.

Recently, transcriptome sequencing has been popular and widely used to explore the molecular mechanism, which was applied to identify the genes and functional pathways involved in the development of cardiac hypertrophy [10]. A hallmark of pathological hypertrophy is significant alterations in the myocardial transcriptome, including mRNA, miRNAs, long non-coding RNAs, and other RNA types, suggesting that interference with transcriptome homeostasis is closely related to disease processes. Hypoxia may lead to different biological processes change in the level of mRNA and protein, affecting the progression of cardiomyocyte hypertrophy and myocardial injury in final. We found that p38-MAPK signaling pathway and HIF-1 signaling pathway have been activated, and cardiomyocyte apoptosis also aggravated, which might be one cause of cardiomyocyte hypertrophy and myocardial injury, and might reveal one treatment and prevention of cardiomyocyte hypertrophy and myocardial injury induced by hypoxia.

2. Materials and Methods

2.1. Experimental Animals and Treatment

Army Military Medical University, the Experimental Animal Center, provided 8–10 weeks (200 ± 20 g) male Sprague-Dawley rats. They were kept at 25°C, with 45% humidity, and exposed to a 12 h light and 12 h dark cycle. They were randomly divided into 4 groups and fed under normoxia (21% O_2) or hypobaric hypoxia (10.0% O_2). The altitude of 5800 m was selected, where hypoxia group was exposed for 7 days, 14 days and 28 days, and the normoxia control group was kept at altitude of 300 m with the normal atmosphere. Isoflurane was used to narcosis after the hypoxia treatment. All procedures observed strictly the standards of experimental animal ethics.

2.2. Measurement of Cardiac Function

Cardiac function was measured in rats anesthetized with isoflurane, briefly, the catheter was inserted into the jugular vein, and guided into the right ventricle, then hemodynamic data were measured, include RVSP (Right Ventricular Systolic Pressure), max dp/dt and min dp/dt [11,12], heart rate (HR), right ventricular end-diastolic pressure (RVEDP), pulmonary artery systolic pressure, mean pulmonary artery pressure. The right ventricle and the left ventricle plus interventricular septum were separated and weighed respectively to calculate RV/(LV+S) as right ventricular hypertrophy index.

2.3. Haematoxylin and Eosin (HE) Staining and Wheat Germ Agglutinin (WGA) Staining

The hearts were fixed with 4% paraformaldehyde over 24h, then sliced into 3 μm after paraffin embedding, the hearts were. To evaluate the cardiomyocyte hypertrophy, haematoxylin and eosin (HE) and fluorescein-conjugated wheat germ agglutinin (WGA) were applied to the slides [13–16]. The slices were incubated with 5.0 μg/mL WGA Alexa Fluor 488 conjugate antibodies for 30 min at 37 ℃. The HE and WGA slides were observed and captured t with Olympus OlyVIA (Olympus, IX-70, Tokyo, Japan) and Case Viewer software (NIKON, DS-U3, Japan). Each HE-stained and WGA-stained section were randomly captured at least ten fields of view, and the myocardial cross-sectional area was calculated with ImageJ software to evaluate morphological changes and cardiomyocyte sizes.

 doi:10.20944/preprints202302.0276.v1

2.4. Transcriptome Sequencing

The hearts tissues of rats were isolated, and each group had three duplicate samples. This sequencing was performed by PTM BIO (Hangzhou, China). Based on the quantitative results, results were final analyzed using Venn analysis, GO enrichment analysis, and KEGG enrichment analysis, functional enrichment analysis, cluster analysis, and Reactome enrichment analysis. Each group had three duplicate samples for sequencing, and only two samples for show.

2.5. Western Blot

The hearts tissues of rats were isolated and washed with pre-cooled PBS, and the right ventricle were homogenized in the radio immunoprecipitation (RIPA) lysis buffer (Beyotime Biotechnology, P0013B, China). The total protein concentration was detected with BCA Protein Assay Kit (Beyotime Biotechnology, P0010, China), and 30 μg of each sample were separated on 4-20% SurePAGE gel (Genscript, M00657, United States) and transferred to 0.45 μm polyvinylidene difluoride (PVDF) membrane (Millipore, IPVH10100, Germany). The primary antibodies as follows: anti-Vinculin antibody (Abcam, ab130007, United States), anti-p38α/β antibody (Santa Cruz Biotechnology, sc-7149, United States), anti-p-p38(Tyr182) antibody (Santa Cruz Biotechnology, sc-7149, United States), anti-Erk1/2 antibody (Santa Cruz Biotechnology, sc-292838, United States), anti-p-Erk1/2 antibody(Santa Cruz Biotechnology, sc-23759-r, United States), anti-C-fos antibody (Abcam, ab190289,), anti-Phospho-c-Fos (Ser32) antibody (Cell Signaling Technology, 5348T, United States), anti-myc antibody (Santa Cruz Biotechnology, Sc-40, United States), anti-p-myc antibody (Santa Cruz Biotechnology,sc-377551, United States), anti-JNK1/2/3 antibody (Abbkine, ABP51664, United States), JNK1/2/3 phospho Thr183/Y185 antibody (Abbkine, ABP50351, United States), anti-c-jun antibody (Santa Cruz Biotechnology, sc-74543, United States), anti-p-c-jun antibody (Santa Cruz Biotechnology, sc-822, United States), anti-HIF-1α antibody (Cell Signal Technology, 36169T, United States), anti- HIF-2α antibody (Cell Signaling Technology, ab199, United States), anti-Bcl-2 antibody (Cell Signaling Technology, 2876S, United States), anti-Bax antibody (Cell Signaling Technology, 2772S, United States), anti-Cytochrome c antibody (Cell Signaling Technology, 4280T, United States), anti-caspase-3 antibody (Cell Signaling Technology, 14220T, United States), anti-cleaved caspase-3 antibody (Abcam,9664S, United States). Then blocking with 5% (w/v) non-fat dry milk at room temperature for 1 h, incubated with primary antibodies overnight at 4°C. The membrane was then rinsed with the TBST buffer and supplemented with the horseradish peroxidase (HRP)-labeled secondary antibody at room temperature for 1 h. Chemiluminescence (ECL) detection kit (KeyGEN BioTECH, KGP1127, China) was adopted to visualize antibody binding, and the Bio Rad Image Lab Software was used to captured the images. The gray value was quantified the bands with ImageJ (version 1.8.0_172). The relative expression of the target proteins was ratio to the control band intensity of the vinculin.

2.6. Statistical Analysis

All data are expressed as mean ± SEM (standard error of the mean), all statistical analyses were performed by using SPSS 26.0. One-way analysis of variance (ANOVA) followed by Tukey's multiple comparison test was used for multiple comparisons. Differences were considered statistically significant at $P < 0.05$.

3. Results

3.1. Hypoxia Developed Pulmonary Hypertension, Right Ventricular Diastolic and Systolic Functions Were Enhanced in Rats

We confirmed HPH using terminal right heart catheterization in rats (**Figure 1**), the systolic pressure of pulmonary artery in H14 ($P < 0.05$) and H28 ($P < 0.01$) were significantly higher than that in control (**Figure 1A**); and the mean pulmonary artery pressure in H14 and H28 were significantly higher than control ($P < 0.01$) (**Figure 1B**). We found significant enhancement of right ventricular systolic function in H14; the max pressure of right ventricular in H14 ($P < 0.05$) and H28 ($P < 0.01$)

Preprints (www.preprints.org) | NOT PEER-REVIEWED | Posted: 16 February 2023 doi:10.20944/preprints202302.0276.v1

were significantly higher than that in control (**Figure 1C**); and the mean right ventricular pressure in H28 ($P < 0.01$) was significantly higher than control **(Figure 1D**). The heart rate of H14 was significantly higher than control ($P < 0.01$) and H7 ($P < 0.05$), H28 was significantly lower than control ($P < 0.01$) and H14 ($P < 0.01$) (**Figure 1E**); the max dp/dt in H14 ($P < 0.05$) and H28 ($P < 0.01$) were significantly higher than control (**Figure 1F**). The min dp/dt in H14 ($P < 0.05$) and H28 ($P < 0.01$) were significantly lower than control (**Figure 1G**); The average dp/dt in H28 ($P < 0.01$) was significantly lower than C. The max min pressure of H28 ($P < 0.01$) was significantly higher than control and H7 (**Figure 1H**); the Tau in H14 ($P < 0.05$) and H28($P < 0.05$) were significantly lower than control (**Figure 1I)**; the IRP average dp/dt in H28 and H14 were significantly lower than control ($P < 0.01$, **Figure 1J**).

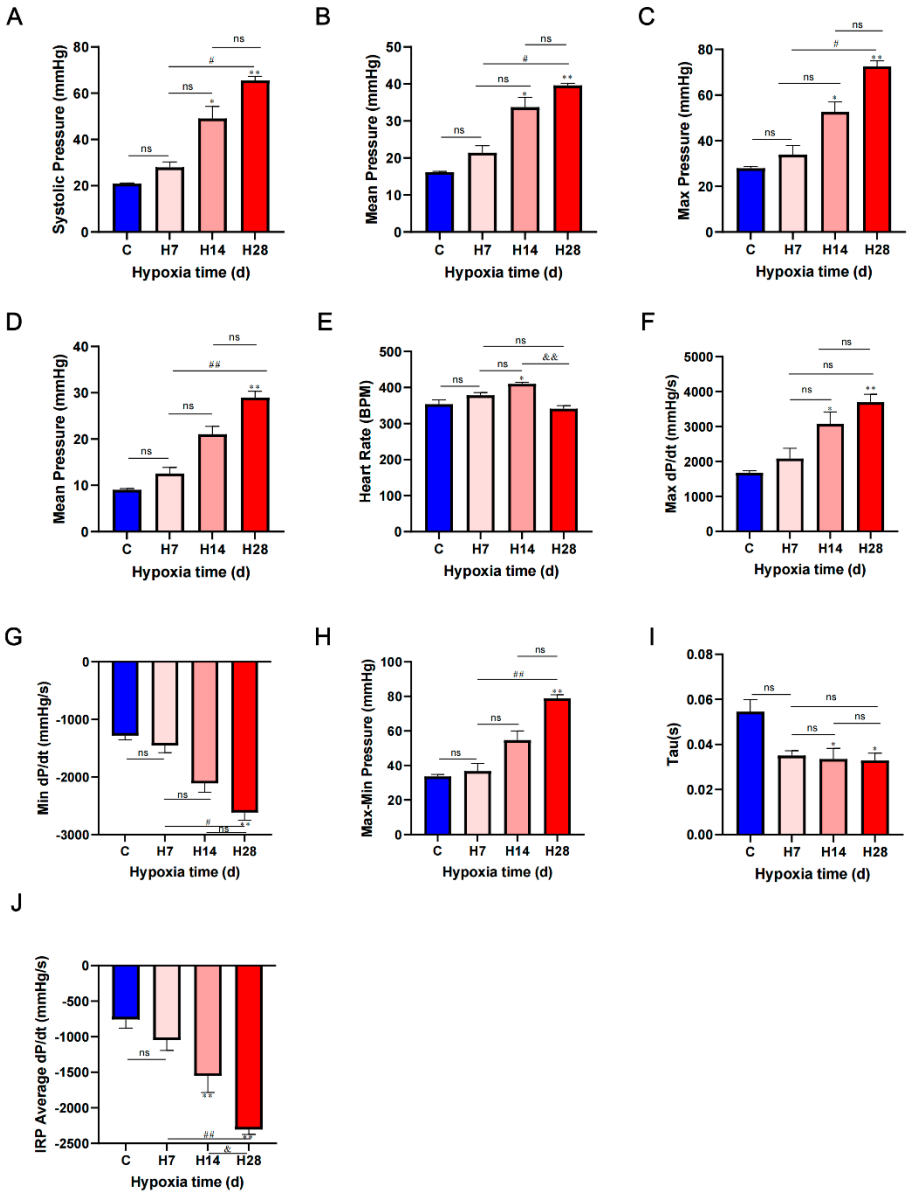

Figure 1. Hypoxia caused elevated pulmonary artery pressure and heart-related loss of function. C=control group, H7, H14 and H28 represent 7, 14 and 28 days of hypoxia, respectively. (A) Systolic pressure of pulmonary artery. (B) Mean pulmonary artery pressure. (C) Max pressure of right ventricular. (D) Mean right ventricular pressure. (E) Heart rate. (F) Maximal of right ventricular pressure rising rate. (G) Maximal of right ventricle diastolic pressure change (H) Max-min pressure of right ventricular. (I) Tau of ventricular pressure. (J) IRP average dp/dt of right ventricular. Data are presented as mean ± SEM; one-way ANOVA; n=6. *$P < 0.05$, ** $P < 0.01$, compare with the control group; #$P < 0.05$, ## $P < 0.01$, compare with the H7; & $P < 0.05$, && $P < 0.01$, compare with the H14.

Preprints (www.preprints.org) | NOT PEER-REVIEWED | Posted: 16 February 2023 doi:10.20944/preprints202302.0276.v1

3.2. Hypoxia Caused Cardiomyocyte Hypertrophy

It can be seen from the general picture of the heart and HE staining (**Figure 2A**) results that the right ventricle was significantly thickened with the prolongation of hypoxia time, the volume of cardiomyocytes in control was smaller, and the outlines of the myocardial fibers were relatively regular. The right heart hypertrophy index (RV/LV+S) and HW/BW of H14 and H28 were significantly higher than control ($P < 0.01$, **Figure 2B,C**). The size of cell size dyeing with WGA is an effective indicator of cardiac hypertrophy [17,18]. Compared with the control and H7, the cardiomyocytes in H14 and H28 were enlarged, the myocardial fiber outline was irregular and deformed, and the myocardial cell cross-sectional area was significantly increased in H14 and H28 dying with HE and WGA ($P < 0.01$, **Figure 2D,E**).

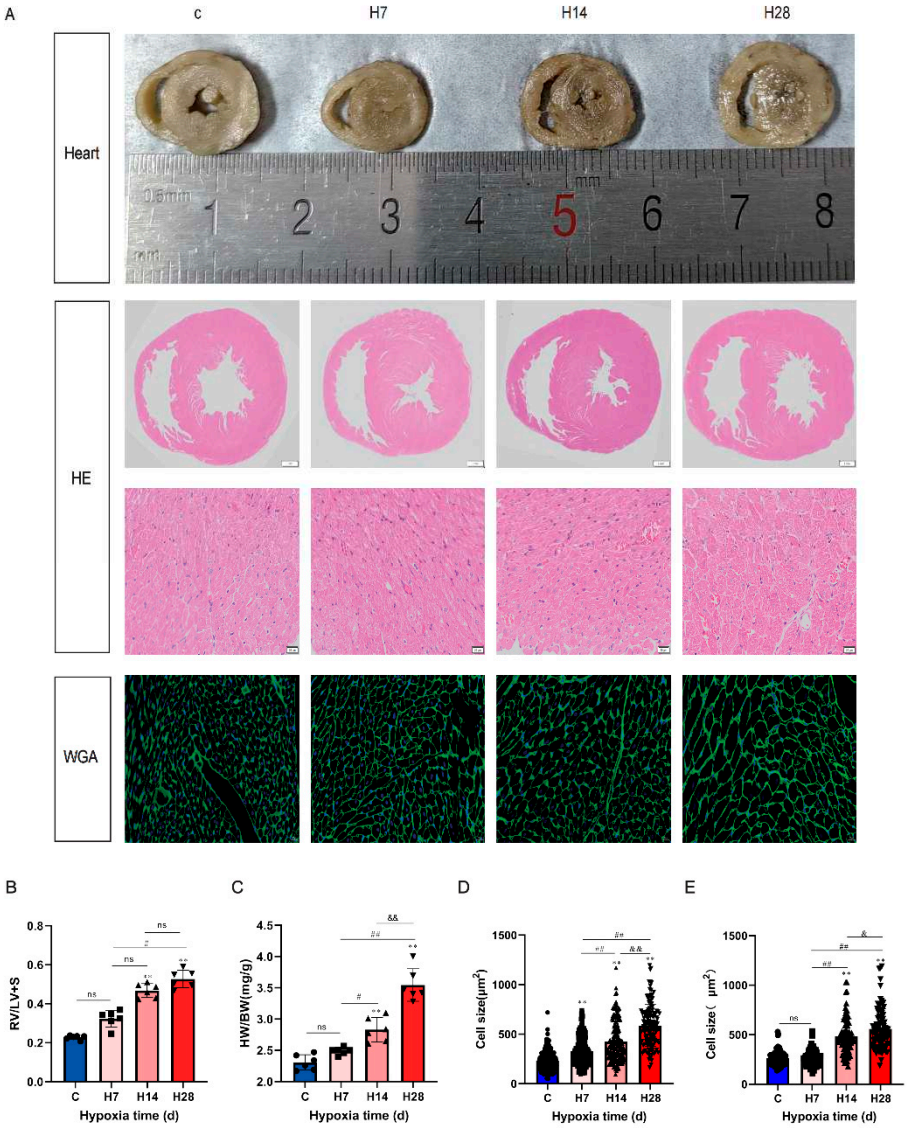

Figure 2. Hypoxia caused cardiac hypertrophy. (A) Representative gross appearance of hearts, heart cross-sections stained with haematoxylin-eosin (scale bar,1mm and 20 μm, magnificationa 1× and 200×), cell boundaries demarcated with fluorescein isothiocyanate-wheat germ agglutinin (scale bar, 20 μm, magnification 400×) and (B) The ratio of right heart weight to left heart weight and ventricular septum (RV/LV+S). n = 6 rats from left to right. (C) The ratio of heart weight to body weight. (D) Statistical results for the cell cross-sectional area with H.E, n = 3. (E) Statistical results for the cell cross-sectional area with WGA, n = 3. Data are presented as mean ± SEM; one-way ANOVA. WGA, wheat germ agglutinin. *$P < 0.05$, ** $P < 0.01$, compare with the control group; #$P < 0.05$, ## $P < 0.01$, compare with the H7; & $P < 0.05$, && $P < 0.01$, compare with the H14.

Preprints (www.preprints.org) | NOT PEER-REVIEWED | Posted: 16 February 2023 doi:10.20944/preprints202302.0276.v1

3.3. Transcriptomic Screening of Right Ventricular

To explore the mechanism of hypoxia on myocardial hypertrophy, transcriptomic screening was performed in right heart tissue of rats. Principal component analysis (PCA) and hierarchical clustering analysis demonstrated robust separation of 4 groups, H28 highly correlated with the control (**Figure 3A,D**), spearman correlation showed similar results (**Figure 3B**). To determine the relationship between 5 comparison groups, we compared the comparison groups of control vs H7, control vs H14, control vs H28, H7 vs H28 and H14 vs H28, compared with the control, 681 genes were changed in the H7; 588 genes were changed in the H14; 76 genes were changed in the 28-day hypoxia group. There were only 3 genes overlap among transcriptomes of these 5 comparison groups (**Figure 3C**).

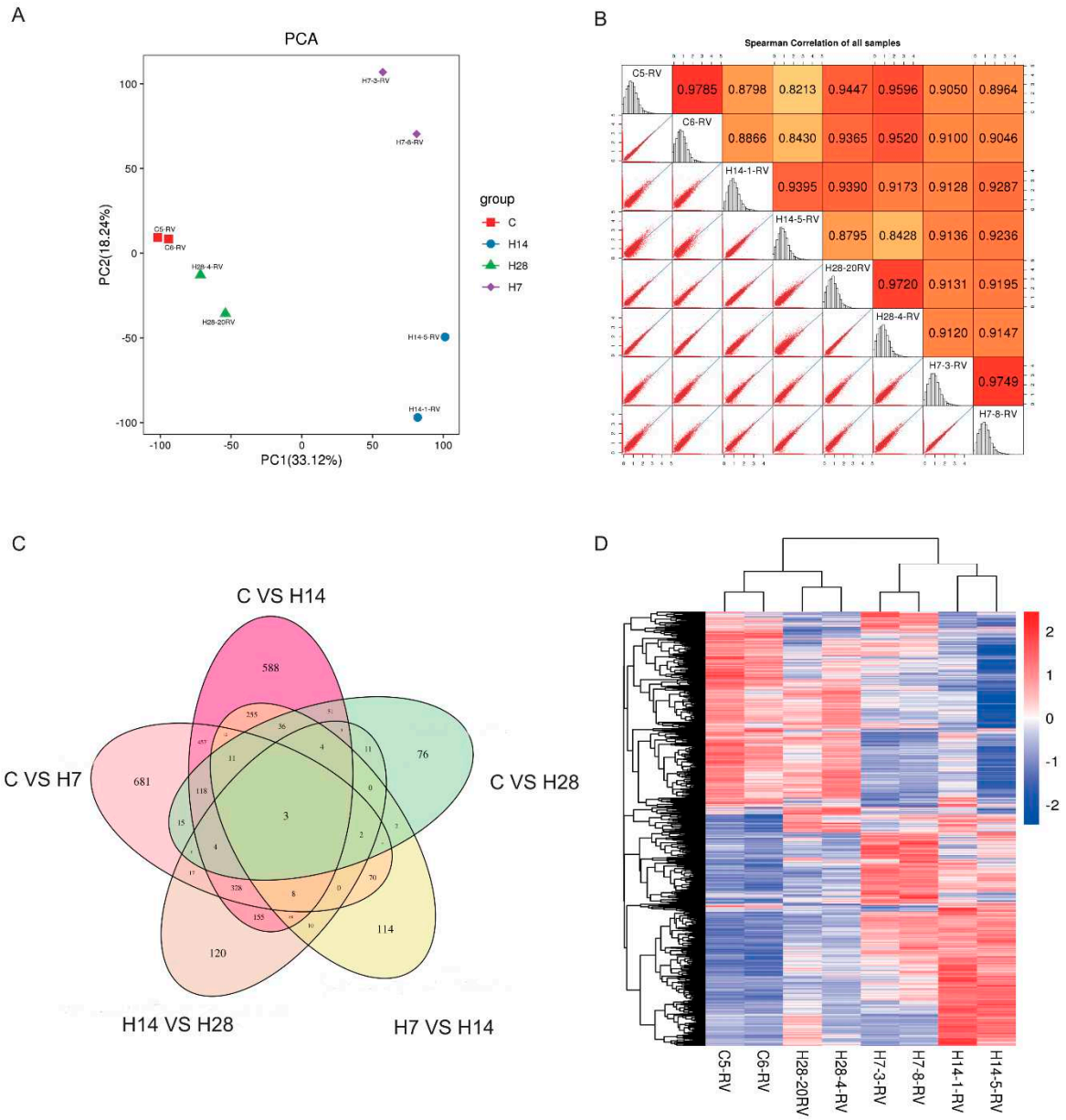

Figure 3. Basic data of right ventricular transcriptome sequencing. (A) Principle component analysis (PCA) of the up-regulation and down-regulation of gene expression in the H7, H14 and H28 compared with the C. (B) Spearman Correlation of all samples. (C) Venn diagrams show the overlap of differentially expressed genes between groups shown. It shows the number of differentially expressed genes. (D) Heat map and clustering analysis of 4 groups (red, upregulated; blue, downregulated).

Preprints (www.preprints.org) | NOT PEER-REVIEWED | Posted: 16 February 2023 doi:10.20944/preprints202302.0276.v1

3.4. The HIF-1 Signaling Pathway and MAPK Signaling Pathway Were Activated by Hypoxia

We selected the major pathways of cardiovascular disease and showed their detailed relationships (Log2 FC > 4) using a Circos diagram (**Figure 4A**). Pathway analysis mainly involved PI3K-AKT signaling pathway, Adrenergic signaling pathway, Calcium signaling pathway, MAPK signaling pathway, FOXO signaling pathway, HIF-1 signaling pathway, etc. the HIF-1 signaling pathway and MAPK signaling pathway were mainly and significantly activated after hypoxia (**Figure 4A**). To verify whether the HIF-1 signaling pathway and MAPK signaling pathway were activated after hypoxia, we verified the key molecules of hif1α, hif2α and MAPK pathway (p38, JNK and ERK).The results showed that HiF-1α ($P < 0.01$) increased significantly with the extension of hypoxia time (**Figure 4B,C**), Hif2α ($P < 0.05$) increased significantly in H7 (**Figure 4D**), ERK and JNK did not change significantly, the phosphorylation of p38 and c-fos increased significantly after H28 (**Figure 4E,F**), indicating the p38 signaling pathway and HIF signaling pathway were activated after hypoxia.

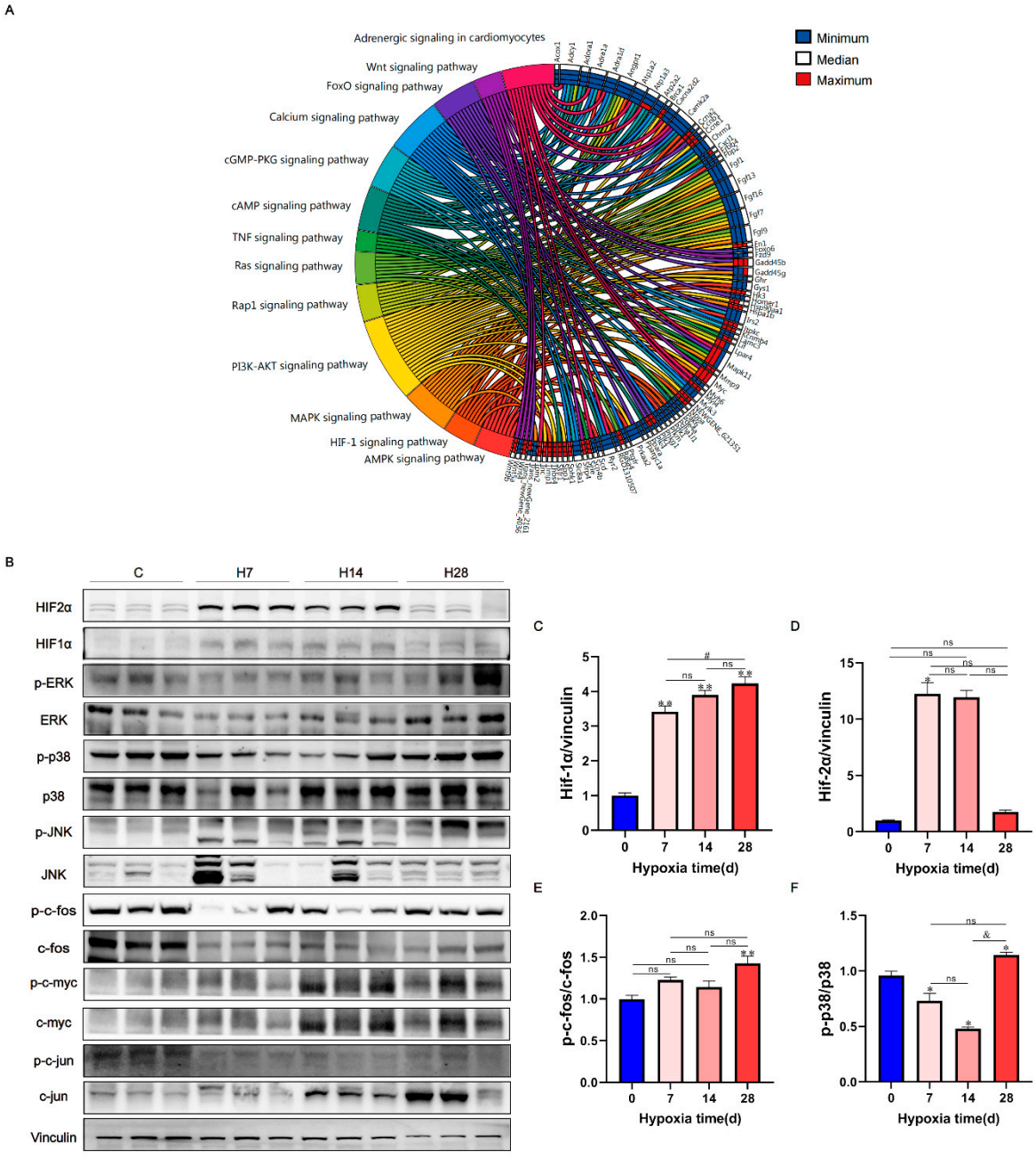

Preprints (www.preprints.org) | NOT PEER-REVIEWED | Posted: 16 February 2023 doi:10.20944/preprints202302.0276.v1

Figure 4. KEGG analysis elucidated cardiac regulatory mechanisms of hypoxia. (A) Detailed relationship between differentially expressed genes and major pathways annotated by KEGG are shown by Circos graph. Differentially expressed genes were chosen to be shown in the right side of the graph. Representative signaling pathways were shown in the left side. For each gene,4 squares and different colors were used to represent the expression levels of 4 sample groups. (B) The representative figures of western blot were shown, and used to measure the protein level of MAPK signaling pathway and HIF signaling pathway proteins. (C)-(F) Ratio results of HIF1α and HIF2α to vinculin, p-c-fos to c-fos, and p-p38 to p38 in right ventricle. Data are presented as mean ± SEM; one-way ANOVA; n = 3. *P < 0.05, **P < 0.01, compare with the control group; & P < 0.05, compare with the H14.

3.5. Apoptosis Occurred in Hypoxic Right Heart Tissue

P38 signaling pathway plays an important role in apoptosis, we used the GSEA database to find the genes in our samples that are significantly changed in the apoptosis pathway (**Figure 5A**). To confirm whether apoptosis occurs in right ventricular after hypoxia, the key molecules of apoptosis, Bax, bcl-2, caspase-3 and Cytochrome C were used for western blot. The results showed that Cytochrome C (***P*** < 0.01) increased significantly in H28 (**Figure 5B,C**), cleaved caspase-3 (**Figure 5D**) and Bax/BCL-2 (***P*** < 0.05) increased significantly in H14 an H28 (**Figure 4F**), it indicated that apoptosis was significantly activated after hypoxia.

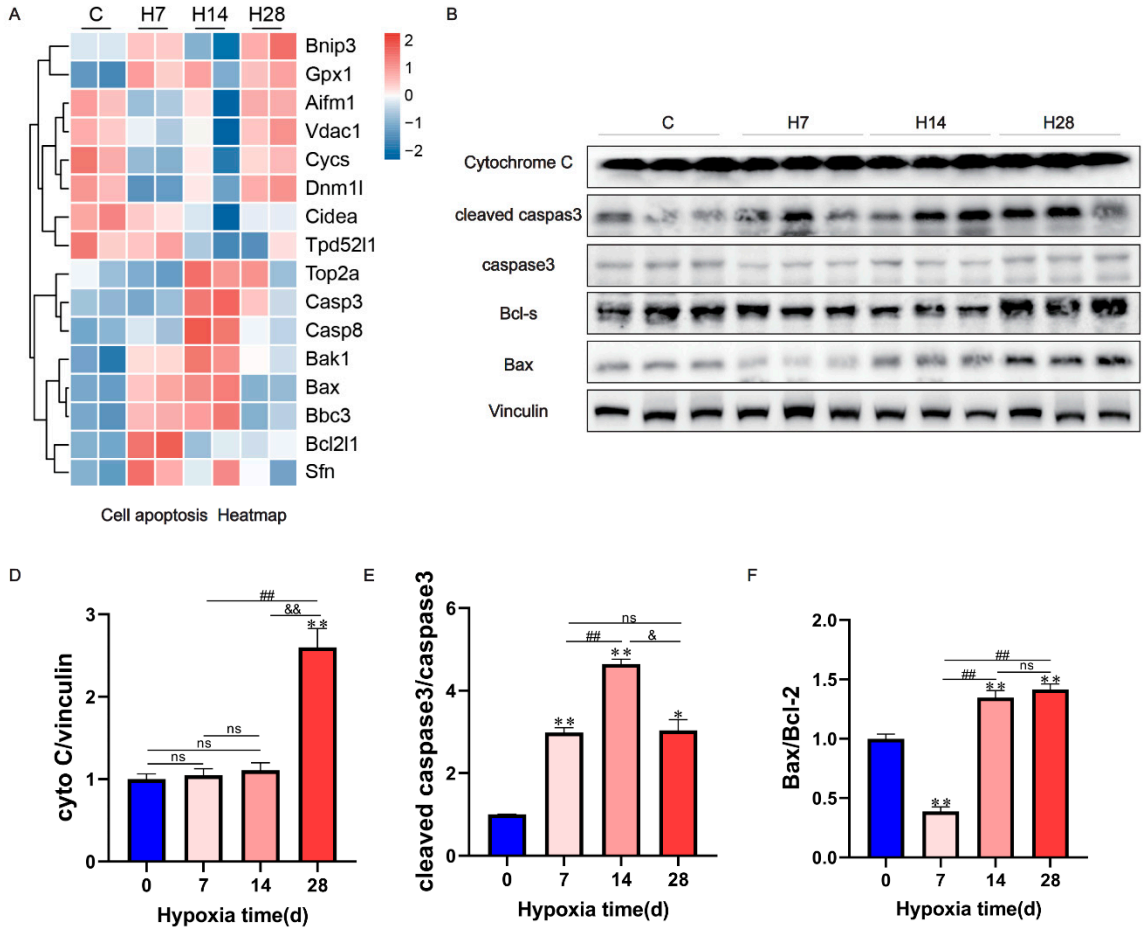

Figure 5. Apoptosis was induced by hypoxia. (A) Heat map of Cell apoptosis. (B) The representative figures of apoptosis signaling pathway proteins were detected by western blot and shown. (C)-(E) Ratio results of cytochrome C to vinculin, cleaved caspase-3 to caspase-3, bax to bcl-2 in right ventricle of rats. Data are presented as mean ± SEM; one-way ANOVA; n = 3. *P < 0.05, **P < 0.01, compare with the control group; #P < 0.05, ## P < 0.01, compare with the H7; & P < 0.05, compare with the H14.

Preprints (www.preprints.org) | NOT PEER-REVIEWED | Posted: 16 February 2023 doi:10.20944/preprints202302.0276.v1

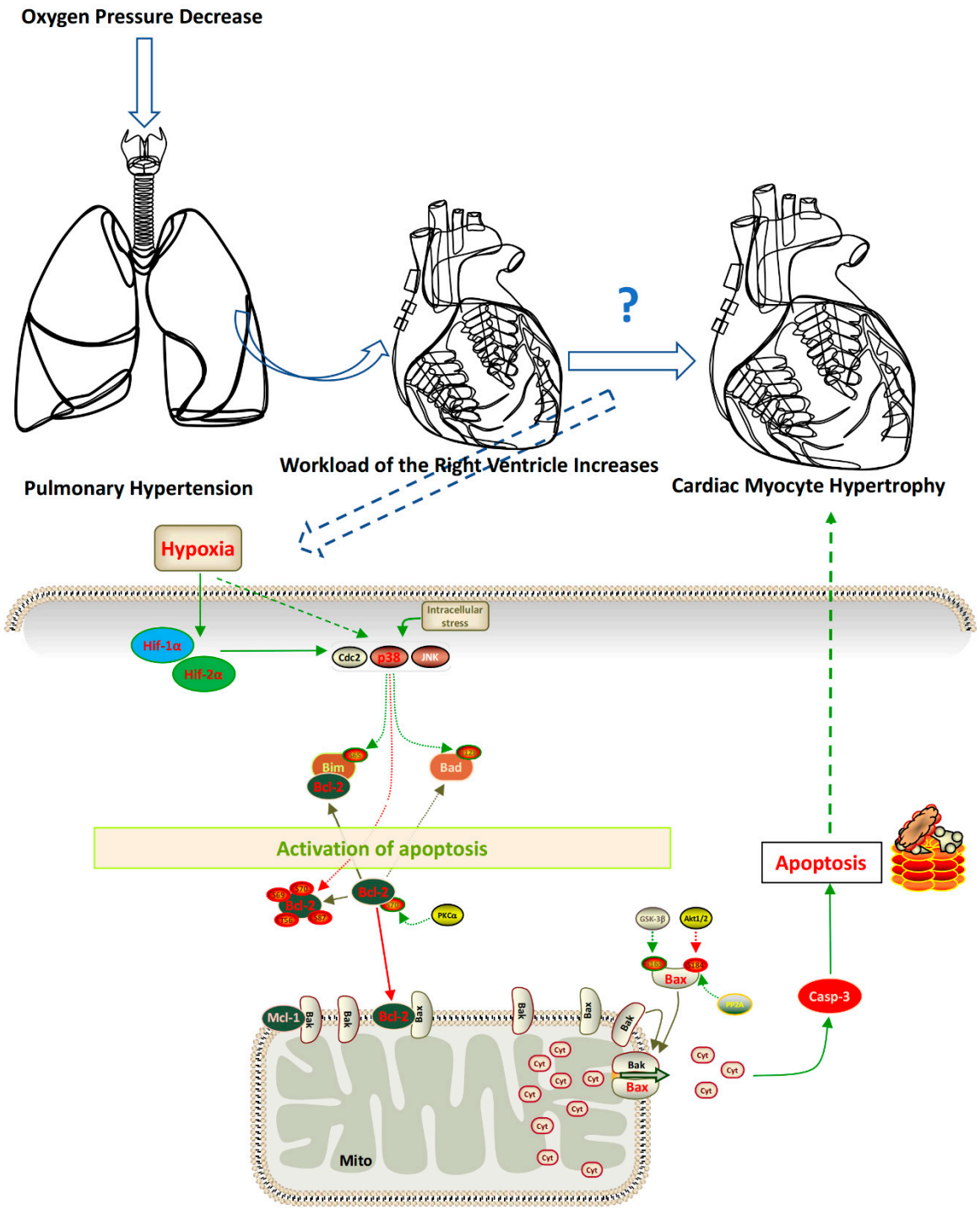

Figure 6. Schematic diagram of the mechanisms underlying apoptosis mediating the cardiac myocyte hypertrophy induced by hypoxia.

4. Discussion

Pulmonary hypertension (PH) is a well-known consequence of the cardio-pulmonary system in high altitude environment, caused by exaggerated hypoxic pulmonary vasoconstriction and even contributes to high altitude pulmonary edema, which occurs at any point 1-5 days following ascent to altitudes ≥2500 m in non-acclimatized healthy individuals [19,20]. Right ventricular failure is life-threatening and the leading cause of death in PH, which can be caused by chronic hypoxia [21,22]. Right ventricular failure is charactered with cardiomyocyte hypertrophy and myocardial injury, with

 doi:10.20944/preprints202302.0276.v1

mortality is high and limited medical therapies, so it`s vital to clarify the underlying mechanisms of cardiomyocyte hypertrophy and myocardial injury induced by chronic hypoxia.

The mechanisms of right ventricular remodeling and failure are complex, pathological features with cardiomyocyte hypertrophy and myocardial injury, and those mechanisms remain unclear. It`s reported that inflammation is pathogenic in PH, and Nrf2 or ERK1/2-Nrf2 signaling pathway may be a target to prevent or reverse PH [23,24]. CD38 inhibits SIRT3 expression and activates of Ca^{2+} -NFAT, playing an essential role in cardiac hypertrophy [25]. Vascular remodeling mediated by NO deficiency and oxidative stress plays a vital role in the pathogenesis of PH, and the total superoxide production and eNOS uncoupling activity induced by hypoxia could be attenuated through netrin-1 and netrin-1 derived small peptides [26]. Oxidative stress-induced myocardial injury and dysfunction can be alleviated by inhibition the calpain of mitochondria in cardiac pathologies, which is an effective strategy [27].

Cardiac hypertrophy is an early hallmark of heart failure, associated with myocardial injury, and cardiomyocyte apoptosis is the main molecular process. Cardiac hypertrophy is initially compensatory for myocardial phenotypic changes, but persistent stress (i.e., apoptosis and fibrosis) makes myocardial function occurs from hypertrophy to failure, in which apoptosis and inflammation play an irreplaceable role. Hypoxia exacerbates cardiomyocyte injury through Wnt3a-Sirt3 and cardiomyocyte apoptosis [28]. Inhibition of integrin ß3 signaling can deteriorate hypoxia injury of cardiomyocytes through inflammatory response, and apoptosis [29]. Resveratrol protected against hypoxia-induced neonatal rat cardiomyocytes injury through regulating Sirt1/p53-mediated apoptosis and NLRP3-mediated inflammation [30].

The p38 mitogen-activated kinase (MAPK) family is closed deeply to cardiac development and function, which controls cell adaptation to stress stimuli, but the mechanism of p38s controlling cardiac physiology and responding to cardiac stress remains limited knowledge [31]. Inhibition of JNK/p38 MAPK signaling pathway retarded myocardial ischemia/reperfusion-induced cardiomyocyte apoptosis in H9C2 cells [32]. Hypoxia and reoxygenation treatment activated NOD2/NOX2/MAPK signaling pathway, which reversed by downregulation of IL-32 expression [33]. Partially inhibition of p38/MAPK signaling pathway also reduces cardiomyocyte apoptosis and improves cardiac dysfunction in myocardial infarction mice [34]. OGD/R-induced cardiomyocyte apoptosis can be prevented through inactivating the MAPK pathway and activating the PI3K/Akt/FoxO and HIF-1α/VEGF pathways [35]. Except molecules, related drug research results are also numerous and outstanding. Curcumin has a protective effect on hypoxia/reoxygenation-induced myocardial injury through via suppression of the MAPK pathway and ER stress [36]. Astragaloside IV regulated of MAPK signaling pathway to prevent apoptosis and restore cardiac function on myocardial infarction in diabetic mice [37].

In this study, we revealed that exposure of rats to 4 weeks of hypoxia induces RV hypertrophy, and we found that the pathway analysis showed a significant change in apoptosis, MAPK, and cardiac hypertrophy. We validated transcriptome data and found that P38-MAPK signaling pathway and HIF-1 signaling pathway were significantly activated, and apoptosis was aggravated. Therefore it`s supposed that apoptosis might play an important role in cardiomyocyte hypertrophy and myocardial injury induced by hypoxia, which might be mediated by the P38 of MAPK signaling pathway. The limitation of this study is also existed, such as the sample size is small, with only 6 animals in each group. The individual differences of animals are large, and the standard deviation between groups is not so good. Therefore, the sample size needs to be further expanded. Second, corresponding cytological experimental verification is poor, and there is only the description of some existing phenomena, lacking of functional studies, so the next step of functional verification is needed to explore in deep.

5. Conclusions

Our findings revealed that cardiac hypertrophy was associated with cardiomyocyte apoptosis in the right ventricular and P38-MAPK signaling pathway and HIF-1 signaling pathway was significantly activated after hypoxia, which might be one cause of cardiomyocyte hypertrophy and

myocardial injury, and targeted intervention of cardiomyocyte apoptosis via P38-MAPK signaling pathway might be one potential prevention for cardiomyocyte hypertrophy and myocardial injury induced by hypoxia.

Author Contributions: J.H. and Z.-J. P.: Conceived and designed the study, D-W. C and L.J.: Reviewing and Editing, X.-X. L., G.X., Y.-D. Y., Y.C., X.-Y. Z., C.-Y. W., Z.-F. Z., S.-M. Z, J.Y., F.-B. S.: performed the experiments and interpreted the data. Z.-J. P.: wrote the manuscript.

Funding: This work was supported by the Military medical science and technology Youth Training program incubation project (20QNPY002), and Army logistics Scientific Research Project- 1226 project (BWS17J031).

Conflicts of Interest: The authors declare no conflict of interest.

References

1. Aaronson, P.I., *Pulmonary hypertension associated with chronic hypoxia: just ASIC-ness?* J Physiol, 2021. **599**(21): p. 4731-4732.
2. Dunham-Snary, K.J., et al., *Hypoxic Pulmonary Vasoconstriction: From Molecular Mechanisms to Medicine.* Chest, 2017. **151**(1): p. 181-192.
3. Zhao, Q., P. Song, and M.H. Zou, *AMPK and Pulmonary Hypertension: Crossroads Between Vasoconstriction and Vascular Remodeling.* Front Cell Dev Biol, 2021. **9**: p. 691585.
4. Xu, X., et al., *Novel Targets in a High-Altitude Pulmonary Hypertension Rat Model Based on RNA-seq and Proteomics.* Front Med (Lausanne), 2021. **8**: p. 742436.
5. Yasukochi, Y., et al., *Transcriptomic Changes in Young Japanese Males After Exposure to Acute Hypobaric Hypoxia.* Front Genet, 2020. **11**: p. 559074.
6. Wang, Y., et al., *Drag-reducing polymers attenuates pulmonary vascular remodeling and right ventricular dysfunction in a rat model of chronic hypoxia-induced pulmonary hypertension.* Clin Hemorheol Microcirc, 2020. **74**(2): p. 189-200.
7. Yang, Z., et al., *Tsantan Sumtang Restored Right Ventricular Function in Chronic Hypoxia-Induced Pulmonary Hypertension Rats.* Front Pharmacol, 2020. **11**: p. 607384.
8. Gao, A.R., et al., *Xinyang Tablet attenuates chronic hypoxia-induced right ventricular remodeling* via *inhibiting cardiomyocytes apoptosis.* Chin Med, 2022. **17**(1): p. 134.
9. Naeije, R., M.J. Richter, and L.J. Rubin, *The physiological basis of pulmonary arterial hypertension.* Eur Respir J, 2022. **59**(6).
10. Zhang, L., et al., *Clinical and translational values of spatial transcriptomics.* Signal Transduct Target Ther, 2022. **7**(1): p. 111.
11. Jayasekera, G., et al., *Understanding longitudinal biventricular structural and functional changes in a pulmonary hypertension Sugen-hypoxia rat model by cardiac magnetic resonance imaging.* Pulm Circ, 2020. **10**(1): p. 2045894019897513.
12. Liu, F., et al., *Isosteviol improves cardiac function and promotes angiogenesis after myocardial infarction in rats.* Cell Tissue Res, 2022. **387**(2): p. 275-285.
13. Baudouy, D., et al., *Echocardiographic and Histological Examination of Cardiac Morphology in the Mouse.* J Vis Exp, 2017(128).
14. Chen, Z., et al., *A simplified herbal formula for the treatment of heart failure: Efficacy, bioactive ingredients, and mechanisms.* Pharmacol Res, 2019. **147**: p. 104251.
15. Yu, J., et al., *Dapagliflozin Mediates Plin5/PPARalpha Signaling Axis to Attenuate Cardiac Hypertrophy.* Front Pharmacol, 2021. **12**: p. 730623.
16. Zhou, Y., et al., *Nobiletin Attenuates Pathological Cardiac Remodeling after Myocardial Infarction* via *Activating PPARgamma and PGC1alpha.* PPAR Res, 2021. **2021**: p. 9947656.
17. Huang, X., et al., *NH(4)Cl treatment prevents doxorubicin-induced myocardial dysfunction in vivo.* Life Sci, 2019. **227**: p. 94-100.
18. Zhang, X., et al., *LuQi Formula Regulates NLRP3 Inflammasome to Relieve Myocardial-Infarction-Induced Cardiac Remodeling in Mice.* Evid Based Complement Alternat Med, 2021. **2021**: p. 5518083.
19. Sydykov, A., et al., *Pulmonary Hypertension in Acute and Chronic High Altitude Maladaptation Disorders.* Int J Environ Res Public Health, 2021. **18**(4).
20. Luks, A.M., E.R. Swenson, and P. Bartsch, *Acute high-altitude sickness.* Eur Respir Rev, 2017. **26**(143).
21. Al-Qazazi, R., et al., *Macrophage-NLRP3 Activation Promotes Right Ventricle Failure in Pulmonary Arterial Hypertension.* Am J Respir Crit Care Med, 2022. **206**(5): p. 608-624.
22. Legchenko, E., et al., *PPARgamma agonist pioglitazone reverses pulmonary hypertension and prevents right heart failure* via *fatty acid oxidation.* Sci Transl Med, 2018. **10**(438).
23. Kang, Y., et al., *Sulforaphane prevents right ventricular injury and reduces pulmonary vascular remodeling in pulmonary arterial hypertension.* Am J Physiol Heart Circ Physiol, 2020. **318**(4): p. H853-H866.

24. Wu, W., Z. Du, and L. Wu, *Dexmedetomidine attenuates hypoxia-induced cardiomyocyte injury by promoting telomere/telomerase activity: Possible involvement of ERK1/2-Nrf2 signaling pathway.* Cell Biol Int, 2022. **46**(7): p. 1036-1046.
25. Guan, X.H., et al., *CD38 promotes angiotensin II-induced cardiac hypertrophy.* J Cell Mol Med, 2017. **21**(8): p. 1492-1502.
26. Murugesan, P., et al., *Novel and robust treatment of pulmonary hypertension with netrin-1 and netrin-1-derived small peptides.* Redox Biol, 2022. **55**: p. 102348.
27. Zheng, D., et al., *Targeted inhibition of calpain in mitochondria alleviates oxidative stress-induced myocardial injury.* Acta Pharmacol Sin, 2021. **42**(6): p. 909-920.
28. Li, Y., et al., *Hypoxia exacerbates cardiomyocyte injury* via *upregulation of Wnt3a and inhibition of Sirt3.* Cytokine, 2020. **136**: p. 155237.
29. Gu, Y., et al., *Neutrophil Gelatinase-Associated Lipocalin2 Exaggerates Cardiomyocyte Hypoxia Injury by Inhibiting Integrin beta3 Signaling.* Med Sci Monit, 2019. **25**: p. 5426-5434.
30. Feng, H., et al., *Resveratrol Inhibits Ischemia-Induced Myocardial Senescence Signals and NLRP3 Inflammasome Activation.* Oxid Med Cell Longev, 2020. **2020**: p. 2647807.
31. Romero-Becerra, R., et al., *p38 MAPK Pathway in the Heart: New Insights in Health and Disease.* Int J Mol Sci, 2020. **21**(19).
32. Zhou, W. and D. Cai, *Midazolam suppresses ischemia/reperfusion-induced cardiomyocyte apoptosis by inhibiting the JNK/p38 MAPK signaling pathway.* Can J Physiol Pharmacol, 2022. **100**(2): p. 117-124.
33. Li, Y. and Z. Wang, *Interleukin 32 participates in cardiomyocyte-induced oxidative stress, inflammation and apoptosis during hypoxia/reoxygenation* via *the NOD2/NOX2/MAPK signaling pathway.* Exp Ther Med, 2022. **24**(3): p. 567.
34. Wang, B., et al., *Kruppel-Like Factor 15 Reduces Ischemia-Induced Apoptosis Involving Regulation of p38/MAPK Signaling.* Hum Gene Ther, 2021. **32**(23-24): p. 1471-1480.
35. Wu, Q., et al., *Multiple pathways are responsible to the inhibitory effect of butorphanol on OGD/R-induced apoptosis in AC16 cardiomyocytes.* J Appl Toxicol, 2022. **42**(5): p. 830-840.
36. Wei, W., J. Peng, and J. Li, *Curcumin attenuates hypoxia/reoxygenation-induced myocardial injury.* Mol Med Rep, 2019. **20**(6): p. 4821-4830.
37. Sun, C., et al., *Astragaloside IV Ameliorates Myocardial Infarction Induced Apoptosis and Restores Cardiac Function.* Front Cell Dev Biol, 2021. **9**: p. 671255.